Two-photon fluorescence excitation spectroscopy by pulse shaping ultrabroad-bandwidth femtosecond laser pulses

Bingwei Xu,[1] Yves Coello,[1] Vadim V. Lozovoy,[1] and Marcos Dantus[1,2,*]

[1]Department of Chemistry, Michigan State University, East Lansing, Michigan 48824, USA

[2]Department of Physics and Astronomy, Michigan State University, East Lansing, Michigan 48824, USA

*Corresponding author: dantus@msu.edu

Received 20 July 2010; revised 10 October 2010; accepted 12 October 2010;
posted 12 October 2010 (Doc. ID 131730); published 9 November 2010

A fast and automated approach to measuring two-photon fluorescence excitation (TPE) spectra of fluorophores with high resolution (~2 nm) by pulse shaping ultrabroad-bandwidth femtosecond laser pulses is demonstrated. Selective excitation in the range of 675–990 nm was achieved by imposing a series of specially designed phase and amplitude masks on the excitation pulses using a pulse shaper. The method eliminates the need for laser tuning and is, thus, suitable for non-laser-expert use. The TPE spectrum of Fluorescein was compared with independent measurements and the spectra of the pH-sensitive dye 8-hydroxypyrene-1,3,6-trisulfonic acid (HPTS) in acidic and basic environments were measured for the first time using this approach.

OCIS codes: 300.6410, 190.7110, 320.5540, 170.2520.

1. Introduction

Simultaneous two-photon absorption (TPA) by an atom or molecule was first predicted by Goeppert-Mayer in 1931 [1], although the first experimental demonstration of this phenomenon had to wait 30 years until the development of lasers [2]. Two-photon spectroscopy has been of interest for studying the electronic structure of molecular excited states [3] because one- and two-photon transitions to a given excited state may have different probabilities depending on molecular symmetry. Two-photon-induced fluorescence has proved very valuable in the biological imaging field. In 1990, Denk *et al.* developed two-photon laser scanning fluorescence microscopy (TPM) [4], a technique that takes advantage of the high photon density required to overcome the low probability for the simultaneous absorption of two photons. Because fluorescence emission via multiphoton excitation occurs only at the beam focus, intrinsic three-dimensional resolution is obtained, out-of-focus background fluorescence is eliminated, and photobleaching is reduced, among other advantages of this microscopy technique over wide-field and one-photon confocal laser scanning fluorescence microscopy [5,6]. Nonlinear optical methods have become widely used tools for medical and biological research and, as a result, commercial two-photon microscopes have been available for a number of years. The two-photon spectra of fluorophores are required to determine which are suitable for this technique and for quantitative TPM studies, and TPA is also becoming relevant for photodynamic therapy [7–9]. The development of new compounds with tailored nonlinear optical properties and well-characterized two-photon spectra is of utmost importance for the development of these applications. Consequently, the measurement of two-photon cross sections has become critically important. For instance, a high two-photon cross section indicates that the compound absorbs a relatively high fraction of the light focused on the

0003-6935/10/326348-06$15.00/0

sample, minimizing possible photodamage to the surroundings.

The techniques commonly used to measure two-photon cross sections of materials can be divided into two groups. One group is based on nonlinear transmission measurements [10–12]. These techniques directly yield the TPA cross section σ_{TPA} and can be applied to nonfluorescent materials, but their implementation is often difficult given that only a very small fraction of photons from the excitation beam is absorbed as it passes through the sample. The second group relies on two-photon-induced fluorescence measurements and provides better sensitivity [13–18]. In most cases, these techniques yield the two-photon fluorescence excitation (TPE) cross section σ_{TPE}, which is directly proportional to the TPA cross section σ_{TPA}, with the constant of proportionality being the fluorescence quantum efficiency η (i.e., $\sigma_{TPE} = \eta\,\sigma_{TPA}$). Although Fourier-transform methods in which the fluorescence sample is placed at the output of a Michelson interferometer have also been reported [19,20], the measurement of TPE spectra has been typically performed by selectively exciting the sample with a narrow-bandwidth laser source, recording the resulting two-photon-induced fluorescence, tuning the laser wavelength, and repeating the process for all the desired wavelengths. Through this approach, a valuable database of TPE spectra of several commercial organic dyes widely used in TPM was reported in the late 1990s, using a tunable femtosecond laser for selective excitation from 690 to ~1000 nm [13,21]. More recently, an extended collection of spectra have been measured in a broader spectral range by using an optical parametric amplifier [18]. Determination of TPE spectra can be significantly simplified by using a standard calibration sample with well-known TPE cross sections. In this case, several measurements of experimental parameters required for absolute cross-section measurements are avoided [21–23].

Broad-bandwidth femtosecond laser sources, including commercial laser oscillators and supercontinua generated in photonic crystal fibers [24], have become more widely available during the past years. TPE spectral measurements can be conveniently obtained using these broad-bandwidth laser sources. Here, we implement a fast and automated approach to measuring the TPE spectra of fluorophores with high resolution using shaped ultrabroad-bandwidth femtosecond laser pulses. This approach eliminates the need for wavelength tuning and is, thus, suitable for non-laser-expert use, especially now that Fourier-transform pulse shapers are commercially available.

2. Experimental

A. Optical Setup

An ultrabroad-bandwidth femtosecond Ti:Al_2O_3 laser oscillator producing ~1.5 nJ pulses at 75 MHz (Venteon Pulse 1, Nanolayers GmbH) was used for the measurements. The spectrum of this laser system spans 620–1050 nm and covers the most relevant two-photon excitation wavelength region of organic dyes. The Fourier-transform pulse shaper used for this work was a folded all-reflective grating-based system consisting of a 150 lines/mm grating, a 762 mm focal length spherical mirror, and a 640 pixel dual-mask spatial light modulator (SLM-640, CRi Inc.). Transform-limited 4.3 fs pulses obtained with this pulse-shaper-enabled femtosecond laser system have been used to generate an ultrabroad-bandwidth second-harmonic generation (SHG) spectrum spanning almost 200 nm in the UV. A more detailed description of this system and its capabilities has been published elsewhere [25,26].

The second-order nonlinear spectrum $S^{(2)}(\omega)$ of the shaped pulses [27] was characterized by measuring the corresponding SHG. For this purpose, the beam from the pulse shaper was focused onto a 20 μm KDP crystal using a 200 mm focal length spherical mirror. The generated SHG beam was then separated from the fundamental beam before directing it to a spectrometer (QE65000, Ocean Optics Inc.) [25]. The spectrometer was calibrated using a tungsten–halogen light source (LS-1-CAL, Ocean Optics Inc.). The SHG spectra were corrected using the spectrometer calibration and the efficiency of the optics present in the SHG separation device described in [25]. These correction factors (not shown) varied less than 10% across the employed bandwidth. The SHG efficiency of the nonlinear crystal [28] was found to be essentially flat across the bandwidth of interest, as demonstrated with experimental and calculated SHG spectra [25,26].

To measure the two-photon-induced fluorescence, the beam from the pulse shaper was focused on the sample solution, which was placed in a 2 mm path length quartz cell, using a 50 mm focal length spherical mirror. The average power of the (spectrally unshaped) pulses at the sample was 10 mW. Note that excitation of the sample is achieved with the fundamental beam via two-photon absorption, while SHG light is only used to characterize $S^{(2)}(\omega)$, as described earlier. The fluorescence was collected at 90° by a 40×, 0.6 NA microscope objective and was then focused on a silicon-avalanche-photodiode-based single photon counting module (SPCM-AQR-12, PerkinElmer) connected to a gated photon counter (Model SR400, Stanford Research Systems). A bandpass filter that allowed the transmission of light in the fluorescence wavelength region (400–600 nm) was also used to filter light from other sources, including scattering of the fundamental pulses. A schematic diagram of the setup is shown in Fig. 1.

For all the experiments, spectral phase distortions of the pulse inherent to the laser and introduced by the optical system were corrected at the sample position by using multiphoton intrapulse interference phase scan (MIIPS). A detailed description of MIIPS and its capabilities has been published elsewhere [26,29]. It is essential to have transform-limited

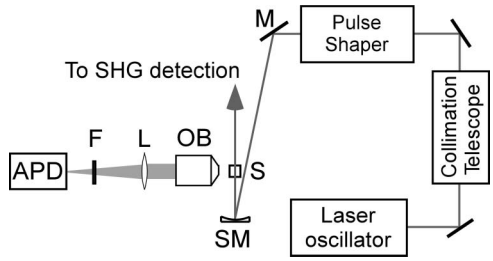

Fig. 1. Experimental setup. The beam from the laser oscillator enters the pulse shaper after a 1:2.5 collimation telescope is used to expand and collimate the beam. The output shaped pulses are focused onto the sample (S), which is either a KDP crystal to generate SHG light or the fluorescent solution, using a spherical mirror (SM). The SHG was separated from the fundamental light and then detected with a spectrometer to characterize the second-order nonlinear spectrum of the shaped pulses. The fluorescence signal was collected with a 40× objective (OB) at 90° and focused onto the APD detection unit with a lens (L). A bandpass filter (F) that allowed the transmission of fluorescence was placed before the detection system.

pulses that have no phase distortions across the entire bandwidth before introducing the amplitude or phase mask that causes selective two-photon excitation at the desired wavelength.

B. Sample Preparation

8-hydroxypyrene-1,3,6-trisulfonic acid (HPTS) 100 μM solutions at pH 6, 7, 8, 9, and 10, and a Fluorescein 100 μM solution at pH 13 were prepared by diluting ~10 mM stock solutions of the dye (Fluorescein and HPTS sodium salts, Fluka) in a buffer at the corresponding pH. Sodium tetraborate (EM Science) was used to prepare 50 mM buffers at pH 9 and 10 ($\pm$0.1), and potassium phosphate monobasic (Mallinckrodt) was used to prepare 50 mM buffers at pH 6, 7, 8, and 13 ($\pm$0.1). The pH of the solutions was measured with a pH meter (Accumet Basic, Fisher Scientific) and adjusted using hydrochloric acid or sodium hydroxide solutions. Deionized water was used in all cases.

3. Results

Two approaches were used to generate shaped pulses able to selectively excite the samples: amplitude and phase shaping. In the amplitude shaping approach, the pulse shaper was used to block all the wavelengths in the fundamental laser spectrum except those in a narrow spectral mask around the desired excitation wavelength. Figure 2(a) shows 60 SHG spectra corresponding to the same number of amplitude masks. For the TPE measurements, the amplitude masks were such that ~10 nm FWHM SHG peaks were generated. In the phase shaping approach, the pulse shaper was used to impose a set of specially designed spectral phases, using specially designed binary sequences (i.e., containing only 0 or π values) with minimum autocorrelation. Details regarding this powerful approach have been published elsewhere [30]. Briefly, the binary phases are built by symmetrizing or antisymmetrizing a minimum-auto-

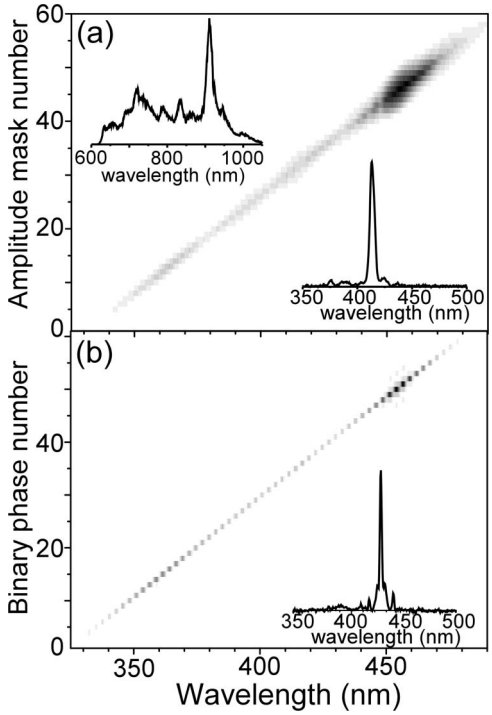

Fig. 2. Selective two-photon excitation by pulse shaping ultrabroad-bandwidth femtosecond laser pulses. In this experiment, the goal was to generate narrow-bandwidth second-order nonlinear spectra suitable for selective two-photon excitation. Experimental SHG spectra were used to characterize the second-order nonlinear spectra of the shaped pulses. (a) 2D contour plot showing SHG spectra obtained by amplitude shaping. The top left plot shows the fundamental (unshaped) spectrum of the laser. The lower right plot shows an example SHG spectrum obtained with amplitude shaping. (b) 2D contour plot showing SHG spectra obtained using binary phase shaping. The lower right plot shows an example SHG spectrum obtained with binary phase shaping. In all cases, spectral intensities are shown in linear scale. In the contour plots, darker regions correspond to higher spectral intensities.

correlation binary sequence around the desired excitation frequency ω_c, i.e., making $\varphi(\omega_c - \omega) = \pm\varphi(\omega_c + \omega)$. As a result, the second-order nonlinear signal is maximized at $2\omega_c$ and minimized everywhere else due to constructive and destructive multiphoton intrapulse interference, respectively. For these experiments, a symmetrized 13 bit binary sequence was used and the whole 26 bit sequence expanded over ~95 nm in the fundamental spectrum. The remaining spectrum was blocked as it does not contribute to increasing the signal at the desired excitation frequency, but only increases the background. The SHG spectra corresponding to 60 binary phases are shown in Fig. 2(b). In this case, the SHG peaks are sharper (~2 nm FWHM) and are, thus, expected to provide higher resolution for TPE spectral measurements.

The TPE spectra were obtained as follows. For each amplitude or phase mask centered at wavelength λ, the resulting two-photon-induced fluorescence intensity $F(\lambda)$ was recorded and the relative cross section $\sigma_{\mathrm{TPE}}(\lambda)$ was calculated according to $\sigma_{\mathrm{TPE}}(\lambda) = F(\lambda)/S^{(2)}(\lambda)$, where $S^{(2)}(\lambda)$ is the integrated

intensity of the corresponding SHG spectrum [31]. Absolute cross sections, which are typically expressed in Goeppert-Mayer units ($1\,\mathrm{GM} = 10^{-50}\,\mathrm{cm}^4\,\mathrm{s/photon}$), were obtained by comparison with Fluorescein as a calibration standard [21].

Figure 3 shows a comparison of the TPE spectrum of Fluorescein measured with this method and independently measured with a tunable laser source [18,21]. The TPE spectra measured with amplitude and binary phase shaping is shown in Figs. 3(a) and 3(b), respectively. Our measurements agree well with the spectrum reported in [21] (squares). Note, however, that the binary phase approach resolves the structure present in the peak at 775 nm. Interestingly, this structure also appears in the spectrum reported in. [18] (triangles).

The fluorescent dye HPTS, also commonly referred to as Pyranine, exhibits (one-photon) absorption spectra highly dependent on pH. Interestingly, the fluorescence spectra maximum occurs at 515 nm regardless of the pH because the pKa of the excited state decreases dramatically upon photoexcitation, resulting in fast deprotonation. Thus, emission occurs only from the ionized form of the molecule. HPTS is stable, commercially available, highly soluble in various solvents, and its pKa ≈ 7.7 is conveniently near the pH of neutral aqueous solutions. These properties, in addition to its large Stokes shift and high fluorescence quantum yield, make HPTS a useful pH-sensitive probe molecule [32,33]. Nevertheless, HPTS pH-dependent TPE spectra have not been reported yet.

The TPE spectra of HPTS at pH 6 and 10 are shown in Figs. 4(a) and 4(b), respectively. The

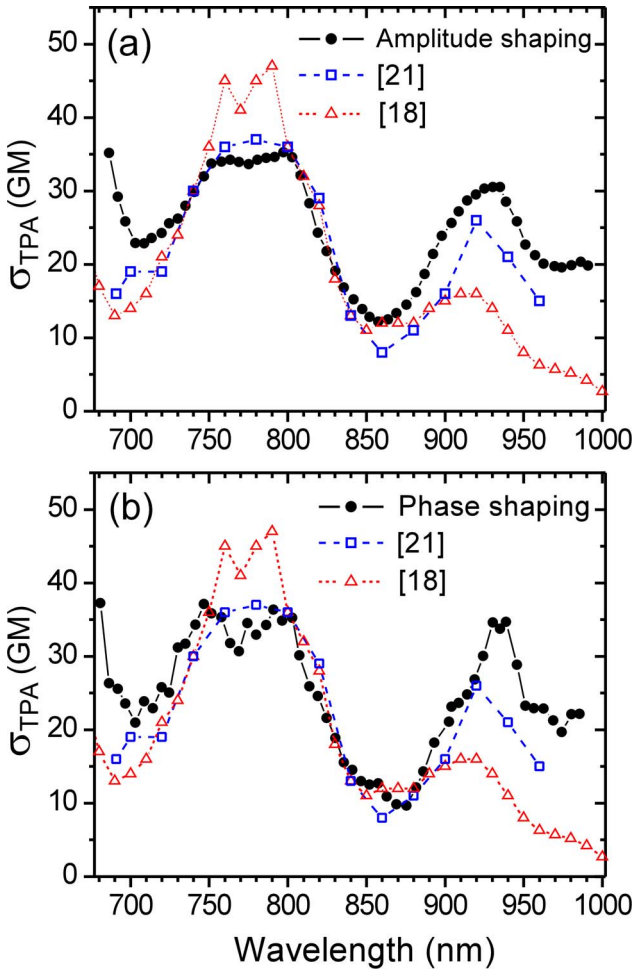

Fig. 3. (Color online) TPE spectrum of Fluorescein at pH 13. The spectra measured by amplitude and binary phase shaping is shown in (a) and (b), respectively, together with independent measurements reported in the literature.

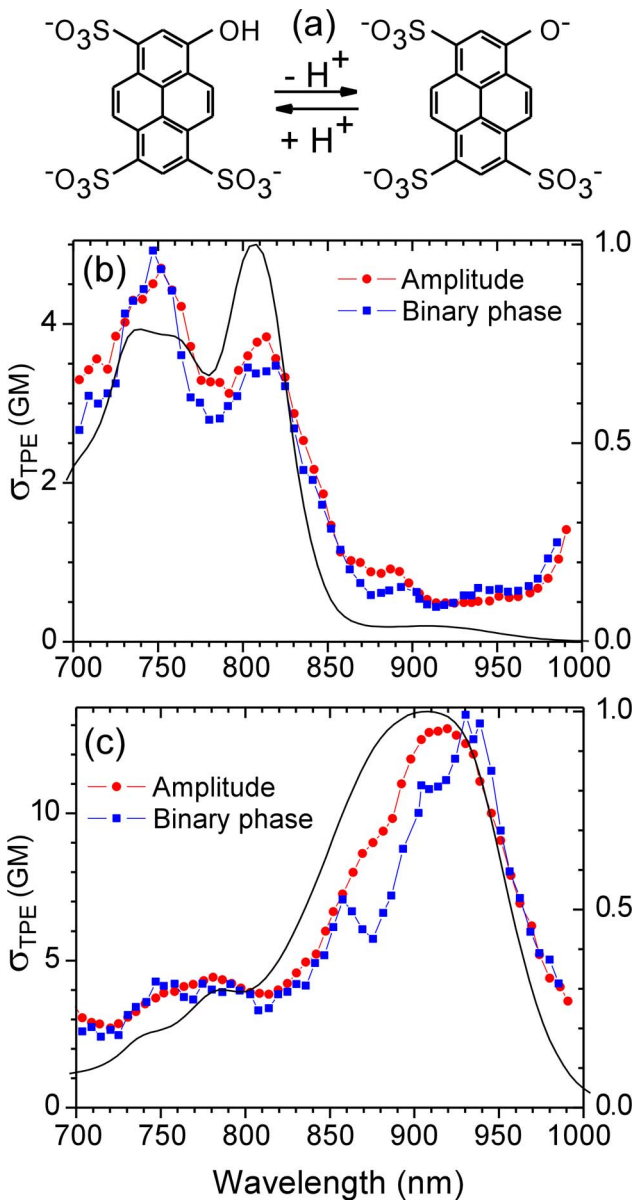

Fig. 4. (Color online) TPE spectra of HPTS in acidic and basic aqueous environments. (a) Acid–base equilibrium reaction of HPTS. (b) TPE spectra of HPTS at pH 6 measured with amplitude (circles) and binary phase shaping (squares). (c) TPE spectra of HPTS at pH 10 measured with amplitude (circles) and binary phase shaping (squares). In both figures, the one-photon absorption spectrum is plotted at twice the wavelength for comparison (solid curve).

one-photon absorption spectra are also plotted at twice the wavelength for comparison (black curve). In this case, a good correlation between the one- and the two-photon transitions exists for the peaks at 750, 810 (pH 6), and 910 nm (pH 10). Note that, in the pH 10 spectra, the shoulder at 875 nm in the spectrum measured with amplitude shaping is clearly resolved in the spectrum taken with binary phase shaping.

The uncertainty in our relative cross-sectional measurements is typically lower than 5%. The uncertainty in the reported absolute cross sections is higher as it also depends on the absolute cross-sectional precision of the employed fluorescence standard (Fluorescein), which has been estimated as 30% [21].

4. Discussion

Given that selective two-photon excitation is accomplished by imposing a set of amplitude and phase masks using an automated pulse shaper, without any change to the excitation source, the approach presented here is significantly faster than conventional approaches based on laser wavelength tuning. The acquisition time for each spectrum was ~2 min, including the time required for SHG characterization, and there are no moving parts.

The wavelength resolution of the presented measurements (~2 nm) is higher than that of most reported TPE spectra measurements (10–20 nm). However, further improvements can be expected. In the amplitude shaping case, narrower amplitude masks would lead to higher resolutions. However, this approach may become experimentally impractical because the energy contained outside the amplitude mask is blocked and, thus, does not contribute to exciting the sample. In that sense, the binary phase shaping approach works more efficiently by concentrating the spectral energy at the desired excitation wavelength while suppressing signal everywhere else in $S^{(2)}(\omega)$. In the binary phase shaping case, the achievable wavelength resolution is limited by the optical resolution of the pulse shaper. Here, ~2 nm FWHM SHG peaks were generated with a symmetrized 13 bit minimum-autocorrelation binary sequence. By using a binary sequence with more bits, the FWHM of the peaks can be reduced to ~1 nm, which corresponds to the optical resolution of our shaper.

As indicated in Section 2, the spectral phase distortions in the optical system, including those introduced by the 40× microscope objective, were corrected at the sample position using MIIPS before applying the desired amplitude or phase mask to the pulses. In the amplitude shaping approach, this procedure ensures that the excitation narrow-bandwidth pulses are transform limited and, thus, that the generated two-photon-induced fluorescence is maximum. Uncorrected spectral phase distortions would reduce fluorescence due to the effect of phase modulation on $S^{(2)}(\omega)$ [34]. In the binary phase shaping approach, spectral phase correction is critical as the generation of sharp peaks in $S^{(2)}(\omega)$ relies on accurate delivery of the binary phases.

5. Conclusions

Selective two-photon excitation by Fourier-transform pulse shaping ultrabroad-bandwidth femtosecond laser pulses was successfully applied to TPE spectroscopy. This pulse shaping approach provides high-resolution two-photon cross-sectional measurements across the ultrabroad-bandwidth of the excitation source without laser tuning. The approach represents a valuable alternative to other available methods as it is also fast and fully automated. The increasing availability of ultrabroad-bandwidth laser sources and pulse shaping devices will facilitate the implementation of the multiphoton cross-sectional measurements as presented here.

We are grateful for a number of fruitful discussions with Dr. Dmitry Pestov from BioPhotonic Solutions Inc. This work was partially funded by the National Science Foundation (NSF) Chemical Research Instrumentation Funds—Instrument Development 0923957.

References

1. M. Goppert-Mayer, "Elementary file with two quantum fissures," Ann. Phys. **9**, 273–294 (1931).
2. W. Kaiser and C. G. B. Garrett, "Two-photon excitation in CaF_2:Eu^{2+}," Phys. Rev. Lett. **7**, 229–231 (1961).
3. M. N. R. Ashfold and J. D. Howe, "Multiphoton spectroscopy of molecular species," Annu. Rev. Phys. Chem. **45**, 57–82 (1994).
4. W. Denk, J. Strickler, and W. Webb, "Two-photon laser scanning fluorescence microscopy," Science **248**, 73–76 (1990).
5. F. Helmchen and W. Denk, "Deep tissue two-photon microscopy," Nat. Methods **2**, 932–940 (2005).
6. A. Diaspro, G. Chirico, and M. Collini, "Two-photon fluorescence excitation and related techniques in biological microscopy," Q. Rev. Biophys. **38**, 97–166 (2005).
7. W. G. Fisher, W. P. Partridge, C. Dees, and E. A. Wachter, "Simultaneous two-photon activation of type-I photodynamic therapy agents," Photochem. Photobiol. **66**, 141–155 (1997).
8. S. Kim, T. Y. Ohulchanskyy, H. E. Pudavar, R. K. Pandey, and P. N. Prasad, "Organically modified silica nanoparticles co-encapsulating photosensitizing drug and aggregation-enhanced two-photon absorbing fluorescent dye aggregates for two-photon photodynamic therapy," J. Am. Chem. Soc. **129**, 2669–2675 (2007).
9. M. K. Kuimova, H. A. Collins, M. Balaz, E. Dahlstedt, J. A. Levitt, N. Sergent, K. Suhling, M. Drobizhev, N. S. Makarov, A. Rebane, H. L. Anderson, and D. Phillips, "Photophysical properties and intracellular imaging of water-soluble porphyrin dimers for two-photon excited photodynamic therapy," Org. Biomol. Chem. **7**, 889–896 (2009).
10. D. A. Oulianov, I. V. Tomov, A. S. Dvornikov, and P. M. Rentzepis, "Observations on the measurement of two-photon absorption cross-section," Opt. Commun. **191**, 235–243 (2001).
11. P. Sengupta, J. Balaji, S. Banerjee, R. Philip, G. R. Kumar, and S. Maiti, "Sensitive measurement of absolute two-photon absorption cross sections," J. Chem. Phys. **112**, 9201–9205 (2000).
12. P. F. Tian and W. S. Warren, "Ultrafast measurement of two-photon absorption by loss modulation," Opt. Lett. **27**, 1634–1636 (2002).

13. C. Xu and W. W. Webb, "Measurement of two-photon excitation cross sections of molecular fluorophores with data from 690 to 1050 nm," J. Opt. Soc. Am. B **13**, 481–491 (1996).
14. C. Xu, J. Guild, W. W. Webb, and W. Denk, "Determination of absolute two-photon excitation cross-sections by in situ second-order autocorrelation," Opt. Lett. **20**, 2372–2374 (1995).
15. P. Kaatz and D. P. Shelton, "Two-photon fluorescence cross-section measurements calibrated with hyper-Rayleigh scattering," J. Opt. Soc. Am. B **16**, 998–1006 (1999).
16. R. Kapoor, C. S. Friend, and A. Patra, "Two-photon-excited absolute emission cross-sectional measurements calibrated with a luminance meter," J. Opt. Soc. Am. B **20**, 1550–1554 (2003).
17. M. Kauert, P. C. Stoller, M. Frenz, and J. Ricka, "Absolute measurement of molecular two-photon absorption cross-sections using a fluorescence saturation technique," Opt. Express **14**, 8434–8447 (2006).
18. N. S. Makarov, M. Drobizhev, and A. Rebane, "Two-photon absorption standards in the 550–1600 nm excitation wavelength range," Opt. Express **16**, 4029–4047 (2008).
19. J. P. Ogilvie, K. J. Kubarych, A. Alexandrou, and M. Joffre, "Fourier transform measurement of two-photon excitation spectra: applications to microscopy and optimal control," Opt. Lett. **30**, 911–913 (2005).
20. K. Isobe, A. Suda, M. Tanaka, F. Kannari, H. Kawano, H. Mizuno, A. Miyawaki, and K. Midorikawa, "Fourier-transform spectroscopy combined with a 5-fs broadband pulse for multispectral nonlinear microscopy," Phys. Rev. A **77**, 063832
(2008).
21. M. A. Albota, C. Xu, and W. W. Webb, "Two-photon fluorescence excitation cross sections of biomolecular probes from 690 to 960 nm," Appl. Opt. **37**, 7352–7356 (1998).
22. G. A. Blab, P. H. M. Lommerse, L. Cognet, G. S. Harms, and T. Schmidt, "Two-photon excitation action cross-sections of the autofluorescent proteins," Chem. Phys. Lett. **350**, 71–77 (2001).
23. S. H. Huang, A. A. Heikal, and W. W. Webb, "Two-photon fluorescence spectroscopy and microscopy of NAD(P)H and flavoprotein," Biophys. J. **82**, 2811–2825 (2002).
24. J. M. Dudley, G. Genty, and S. Coen, "Supercontinuum generation in photonic crystal fiber," Rev. Mod. Phys. **78**, 1135–1184 (2006).
25. B. W. Xu, Y. Coello, V. V. Lozovoy, D. A. Harris, and M. Dantus, "Pulse shaping of octave spanning femtosecond laser pulses," Opt. Express **14**, 10939–10944 (2006).
26. Y. Coello, V. V. Lozovoy, T. C. Gunaratne, B. W. Xu, I. Borukhovich, C. H. Tseng, T. Weinacht, and M. Dantus, "Interference without an interferometer: a different approach to measuring, compressing, and shaping ultrashort laser pulses," J. Opt. Soc. Am. B **25**, A140–A150 (2008).
27. K. A. Walowicz, I. Pastirk, V. V. Lozovoy, and M. Dantus, "Multiphoton intrapulse interference. 1. Control of multiphoton processes in condensed phases," J. Phys. Chem. A **106**, 9369–9373 (2002).
28. A. Baltuska, M. S. Pshenichnikov, and D. A. Wiersma, "Second-harmonic generation frequency-resolved optical gating in the single-cycle regime," IEEE J. Quantum Electron. **35**, 459–478 (1999).
29. B. W. Xu, J. M. Gunn, J. M. Dela Cruz, V. V. Lozovoy, and M. Dantus, "Quantitative investigation of the multiphoton intrapulse interference phase scan method for simultaneous phase measurement and compensation of femtosecond laser pulses," J. Opt. Soc. Am. B **23**, 750–759 (2006).
30. V. V. Lozovoy, B. W. Xu, J. C. Shane, and M. Dantus, "Selective nonlinear optical excitation with pulses shaped by pseudorandom Galois fields," Phys. Rev. A **74**, 041805 (2006).
31. R. D. Jones and P. R. Callis, "A power-squared sensor for 2-photon spectroscopy and dispersion of 2nd-order coherence," J. Appl. Phys. **64**, 4301–4305 (1988).
32. J. M. Dela Cruz, I. Pastirk, M. Comstock, V. V. Lozovoy, and M. Dantus, "Use of coherent control methods through scattering biological tissue to achieve functional imaging," Proc. Natl. Acad. Sci. USA **101**, 16996–17001 (2004).
33. D. B. Spry, A. Goun, C. B. Bell III, and M. D. Fayer, "Identification and properties of the ^1L_a and ^1L_b states of pyranine," J. Chem. Phys. **125**, 144514 (2006).
34. V. V. Lozovoy and M. Dantus, "Systematic control of nonlinear optical processes using optimally shaped femtosecond pulses," Chem. Phys. Chem. **6**, 1970–2000 (2005).